Fish and Shellfish Immunology 84 (2019) 333–340

Contents lists available at ScienceDirect

Fish and Shellfish Immunology

journal homepage: www.elsevier.com/locate/fsi

Full length article

Expression profiling and functional characterization of galectin-3 of turbot (*Scophthalmus maximus* L.) in host mucosal immunity

Mengyu Tian[1], Ning Yang[1], Lu Zhang, Qiang Fu, Fenghua Tan, Chao Li*

Marine Science and Engineering College, Qingdao Agricultural University, Qingdao, 266109, PR China

ARTICLE INFO

Keywords:
Galectin-3
Turbot
Vibrio anguillarum
Streptococcus iniae
Microbial ligand binding

ABSTRACT

Galectins, a family of evolutionary conserved β-galactoside-binding proteins, have been characterized in a wide range of species. Galectin-3 is the only member in the chimera type, which is a monomeric lectin with one CRD domain. A growing body of evidence have indicated vital roles of galectin-3 in innate immune responses against infection. Here, one galectin-3 gene was captured in turbot (*Sm*Lgals3) with a 1203 bp open reading frame (ORF). In comparison to other species, *Sm*Lgals3 showed the highest similarity and identity to large yellow croaker and medaka, respectively. The genomic structure analysis showed that *Sm*Lgals3 had 5 exons similar to other vertebrate species. The syntenic analysis revealed that galectin-3 had the same neighboring genes across all the selected species, which suggested the synteny encompassing galectin-3 region during vertebrate evolution. Subsequently, *Sm*Lgals3 was widely expressed in all the examined tissues, with the highest expression level in brain and the lowest expression level in skin. In addition, *Sm*Lgals3 was significantly down-regulated in intestine following both Gram-negative bacteria *Vibrio anguillarum*, and Gram-positive bacteria *Streptococcus iniae* immersion challenge. Finally, the *rSm*Lgals3 showed strong binding ability to all the examined microbial ligands. Taken together, our results suggested *Sm*Lgals3 played vital roles in fish innate immune responses against infection. However, the knowledge of *Sm*Lgals3 are still limited in teleost species, further studies should be carried out to better characterize its detailed roles in teleost mucosal immunity.

1. Introduction

Galectins, a family of evolutionary conserved β-galactoside-binding proteins, have been characterized in a wide range of species, including fungi, parazoa, and vertebrates [1,2]. The galectins were featured with a characteristic carbohydrate recognition domain (CRD) with an affinity for β-galactosides, and a conserved sequence motif [3]. According to the structural features, galectin family has been classified into three different types: proto-type, Chimera type and tandem-repeat type [4]. As a group of carbohydrate-binding proteins, galectins could involve in many biological processes, such as pathogen recognition, inflammation, cell migration and development [5]. So far, 14 galectin members have been discovered in mammals, but lower vertebrates and invertebrates appear to have a smaller number of galectins. In teleost, several studies have been carried out to characterize galectin genes, since the first galectin gene was identified in electric organs of the electric eel (*Electrophorus electricus*) [6]. For instance, 8 galectins were identified in catfish, and showed significant expression changes following *Edwardsiella ictaluri* and *Flavobacterium columnare* challenge in mucosal tissues [7].

Among three galectin types, only galectin-3 belongs to the chimera type, which is a monomeric lectin with one CRD domain. Similar to the other galectin types, galectin-3 also lacks a signal sequence which is required for secretion, but the galectin-3 protein could be released into the extracellular space [8]. Of note, galectin-3 has been captured in a wide range of immune cells, including mast cells, macrophages, neutrophils, monocytes and T cells. For instance, galectin-3 deletion suppressed production of pro-inflammatory cytokines and significantly reduced activation of NOD-like receptor family in macrophages in mice [9]. In T cells, galectin-3 could induce the production of IL-2 [10], as well the apoptosis in both Th1 and Th2 cells [11]. In teleost species, galectin-3 could reduce the adhesion of infectious hematopoietic necrosis virus by direct interaction with virus envelop on the epithelial cell surface in a carbohydrate-dependent manner [12]. In oyster (*Crassostrea gigas*), galectin-3 displayed agglutination ability against both *Micrococcus luteus* and *Pichia pastoris* [13]. However, most of the studies of galectin-3 were performed in mammals, the characterization of galectin-3 in teleost was still limited in a handful species.

* Corresponding author.
E-mail address: leoochao@163.com (C. Li).
[1] All these authors contributed equally to this work.

https://doi.org/10.1016/j.fsi.2018.10.009
Received 4 August 2018; Received in revised form 12 September 2018; Accepted 5 October 2018
Available online 06 October 2018
1050-4648/

Turbot (*Scophthalmus maximus* L.), one of the most extensively maricultured species in China, suffers from the bacterial disease including *Vibrio anguillarum* and *Streptococcus iniae*. Many studies have been performed to identify the immune-related genes and investigate their associated activities during bacterial infection [14–18], for further development of the disease control and prevention measures in turbot. In this regard, we sought here to characterize galectin-3 gene in turbot, and its expression patterns following different bacterial infection, as well as microbial ligand-binding activities to gain initial insight into the immune roles of galectin-3 in teleost.

2. Materials and methods

2.1. Sequence identification and analysis

The turbot galectin-3 gene was captured from transcriptome database [19] by BLAST program using galectin-3 protein sequences from other species as queries. The retrieved candidate sequences were then translated using ORF Finder (http://www.ncbi.nlm.nih.gov/gorf/gorf.html). The predicted ORF sequences were further verified against NCBI non-redundant protein sequence database by BLASTP (http://blast.ncbi.nlm.nih.gov/Blast.cgi). The conserved domains and signal peptides were further identified by the simple modular architecture research tool (SMART; http://smart.embl-heidelberg.de/). The theoretical pI, molecular mass and N-glycosylation sites were captured in ExPASy server [20]. The intron and exon structures were predicted by Splign program [21].

2.2. Phylogenetic analysis

The phylogenetic tree was constructed based on the amino acid sequences of galectin-3 gene from various species including human (*Homo sapiens*), shrew mouse (*Mus pahari*), chicken (*Gallus gallus*), green sea turtle (*Chelonia mydas*), spotted gar (*Lepisosteus oculatus*), zebrafish (*Danio rerio*), medaka (*Oryzias latipes*), tilapia (*Oreochromis niloticus*), fugu (*Takifugu rubripes*). The multiple protein sequence alignment was performed in Clustal Omega program [22]. A neighbor-joining phylogenetic tree was generated using the Molecular Evolutionary Genetics Analysis (MEGA 6) [23].

2.3. Syntenic analysis

Syntenic analysis was performed to further verify the identification of turbot galectin-3 gene. Briefly, the protein sequences of neighboring genes of the turbot galecin-3 were predicted from the turbot scaffold using FGENESH program. The identified protein sequences were annotated by BLASTP program against NCBI non-redundant (nr) database. The conserved syntenic pattern of galectin-3 gene in other species were characterized in Ensembl database and Genomicus [24].

2.4. Bacteria challenge and sample collection

In order to characterize the roles of galectin-3 gene in the host immune responses against bacterial infection, the Gram-negative bacteria *V. anguillarum* and Gram-positive bacteria *S. iniae* were selected to conduct the immersion challenge. Turbot fingerlings (average body weight: 15.6 g and average body length = 5.5 cm) were obtained from the turbot hatchery (Haiyang, Shandong, China), and acclimated in the laboratory in a flow-through system for at least two weeks prior to challenge. After a pre-challenge, the bacteria was re-isolated from single symptomatic fish and biochemically confirmed before experiment. During the experiment, the experimental fish were challenged for 2 h by immersion, and then transferred in fresh water. At each time-point following challenge, skin, gill and intestine samples were collected from 15 fish (5 fish per pool) from the appropriate aquaria.

Briefly, the *V. anguillarum* was inoculated in LB broth in a shaker (180 rpm) at 28 °C overnight. The fish were immersed at a final concentration of 5×10^7 CFU/mL for 2 h, while the control fish were immersed in sterilized media alone. Aquaria were randomly assigned for 2 h, 6 h, 12 h and 24 h post-treatment and 0 h control with 30 fish in each aquarium for sample collection.

The *S. iniae* isolate was inoculated in LB medium in a shaker incubator at 28 °C overnight. The fish were equally divided into 5 aquariums, 4 challenged groups (2 h, 4 h, 8 h and 12 h) and one control group. For the challenge, the fish were immersed for 2 h at a final concentration of 5×10^6 CFU/mL, while the control fish were immersed in sterilized media alone. All samples from both experiments were flash-frozen in liquid nitrogen and then stored in a −80 °C ultra-low freezer until preparation of RNA.

2.5. Total RNA extraction and cDNA synthesis

Prior to RNA extraction, tissue samples were homogenized under liquid nitrogen using mortar and pestle. Total RNA was extracted using Trizol® Reagent (Invitrogen, USA) according to the supplied protocol. The quality and quantity of RNA of each sample were measured on a Nanodrop 2000 (Thermo Electron North America LLC, FL, USA). All extracted samples had an A260/280 ratio greater than 1.8, and were diluted to 250 ng/μl.

2.6. Real-time PCR analysis

Gene specific primers were designed using Primer3 software based on the turbot galectin-3 sequences, and 18S rRNA gene was used as a reference gene (Table 1). First strand cDNA was synthesized by PrimeScript RT reagent Kit (TaKaRa) according to manufacturer's protocol (500 ng RNA per 10 μl reaction). Quantitative real-time PCR (qPCR) was performed on a CFX96 real-time PCR detection system (Bio-Rad Laboratories, CA, USA) using the SYBR ExScript qRT-PCR Kit (Takara, Dalian, China). The reaction systems for all real-time PCR were as follows: 1.0 μL of each primer (5 μM), 5.0 μL SYBR Green supermix, 2.0 μL RNase/DNase-free water, and 1.0 μl 200 ng/μL cDNA. The PCR reaction mixture was denatured at 95 °C for 30 s and then subjected to 40 cycles of 95 °C for 5 s, 58 °C for 5 s and followed by dissociation curve analysis, 5 s at 65 °C, then up to 95 °C at a rate of 0.1 °C/s increment, to verify the specificity of the amplicons. Results were analyzed using Relative Expression Software Tool (REST) to capture the significance at the level of $P < 0.05$ [25]. In order to determine the gene expression patterns in turbot healthy tissues, the tissue with the lowest Ct values was used as control. The mRNA expression levels of all samples were normalized to the levels of 18S rRNA gene in the same samples. A no-template control was run on all plates.

2.7. Plasmid construction

In order to construct the expression plasmid for *Sm*Lgals3, *Sm*Lgals3 was amplified with the specific primers following cDNA synthetization. After gel extraction, the PCR products were ligated to pEASY-Blunt-E1 vector, and then transformed into competent Trans1-T1 cells. Following

Table 1
Primers used in this study.

Primer	Sequence (5'-3')
qRT-PCR	
Sm-lgals3 F	5′AGGACTGTGAGCGGCTATAC3′
Sm-lgals3 R	5′ACAAAGCCGTACGAGAGACA3′
18s RNA F	5′ATGGCCGTTCTTAGTTGGTG3′
18s RNA R	5′CTCAATCTCGTGTGGCTGAA3′
Protein expression	
Sm-lgals3-pr F	5′ATGGCGGATTTCTCGCTGAC3′
Sm-lgals3-pr R	5′TCAGATCATGCTCGGGGC3′

blue-white spotting selection, the positive clones were selected and sequenced with T7 Promoter Primer. The verified recombinant plasmid was extracted and marked as pEASY-E1- Lgals3.

2.8. Expression and purification of recombinant SmLgals3

The recombinant plasmid pEASY-E1- Lgals3 was transformed into *E.coli* BL21 (DE3). The transformant BL21- Lgals3 and the control BL21 with empty pET-32a were cultured in LB medium, and induced by adding 0.5 mM isopropyl-b-D-thiogalactopyranoside. The expressed protein was purified by nickel-nitrilotriacetic acid chromatography, and analyzed by 12% sodium dodecyl sulfate polyacrylamide gel electrophoresis (SDS-PAGE) and visualized by staining with Coomassie brilliant blue. The concentration of the recombinant protein was determined using Bradford's method.

2.9. Solid-phase enzyme-linked immunosorbent assay (ELISA)

The binding ability of *rSm*Lgals3 with lipopolysaccharide (LPS), lipoteichoic acid (LTA) and peptidoglycan (PGN) was detected by ELISA method. Briefly, LPS/LTA/PGN (5 μg/mL) were coated to 96 microtitor plate at 4 °C overnight. The wells were washed with 300 μl PBST three times, and then blocked with 100 μl 5% BSA at 4 °C for 1 h. Then, 100 μl of increasing concentrations of purified recombinant *Sm*Lgals3 (0.5, 1, 2, 4, 8 and 16 μg/mL) were added into each ligand-coated well, with 4 replicates for each concentration, and incubated at 37 °C for 1 h. Subsequently, the wells were incubated at 37 °C for 1 h with 100 μl mouse anti-His antibody (Solarbio, Beijing, China) (diluted 1:1000 in 5% BSA), followed by another incubation at 37 °C for 40 min with the addition of 100 μl horseradish peroxidase conjugated goat anti-mouse IgG (Solarbio, Beijing, China) (diluted 1:1000 in 5% BSA). Finally, the reaction was terminated by adding 0.5 M sulfate, and the plate was then read at 450 nm with an ELISA reader.

3. Results

3.1. Identification of turbot galectin-3 gene

After searching the turbot transcriptome and genome database [26] using available galectin-3 sequences from other species as queries, one galectin-3 gene was captured in turbot (*Sm*Lgals3). In detail, the full-length *Sm*Lgals3 (GenBank accession: MF797865) transcript contains a 1203 bp open reading frame (ORF) encoding 400 amino acids residues with a predicted molecular mass of a 39.74 kDa and a theoretical isoelectric point of 5.12 (Table 2). The deduced *Sm*Lgals3 protein was predicted to have 1 Casein kinase II phosphorylation sites, as well as 24 negatively charged residues (Asp + Glu), 13 positively charged residues (Arg + Lys), and with an instability index of 54.9 and aliphatic index of 45.42 (Table 2). In comparison to other species, *Sm*Lgals3 showed the highest similarity to large yellow croaker (68%), followed by zebrafish (66.5%), while the highest identity was observed with medaka (61.3%), followed by tilapia (60.1%) (Table 3).

Table 2
Primary structural analysis. Properties of turbot *Sm*Lgals3 gene determined by ProtParam.

Analysis	*Sm*Lgals3
No. of amino acids	400
Molecular weight (kDa)	39.74
Theoretical pI	5.12
Total number of negatively charged residues (Asp + Glu)	24
Total number of positively charged residues (Arg + Lys)	13
Formula	$C_{1814}H_{2637}N_{477}O_{516}S_{11}$
Instability index	54.9
Aliphatic index	45.42
Grand average of hydropathicity (GRAVY)	−0.354
Protein kinase C phosphorylation site	0
Casein kinase II phosphorylation site	1
N-glycosylation site	0

Table 3
Amino acid comparison of *SmLgals3* genes with other species using MatGAT program.

Species	Turbot *lgals3*	
	Similarity	Identity
Turbot *lgals3*		
Human *lgals3*	43.8	35.1
Green Turtle *lgals3*	49.3	38.7
Mouse *lgals3*	45	36
Chicken *lgals3*	42	35.7
Tetraodon *lgals3*	62.3	58.4
Medaka *lgals3*	66.3	61.3
Tilapia *lgals3*	64.3	60.1
Large yellow croaker *lgals3*	68	56.3
Zebrafish *lgals3*	66.5	58.3

3.2. Genomic structure analysis of SmLgals3 gene

Following sequence identification, the genomic architecture of *Sm*Lgals3 was also investigated. Following the comparison of the exon/intron organization of *Sm*Lgals3 with other vertebrates, the N-terminal and C-terminal showed different similarities among the selected species. In detail, the exon number was varied from 5 to 7, and the CRD domain was composed by three same exons (89 bp,166 bp and 156 bp) in all the species (Fig. 1), whereas the different number of exons were observed in their N-terminal domains. In general, there were 5 exons in the mammals and chicken, and more exons (6 and 7) in fish species, except turbot also showed 5 exons (Fig. 1).

3.3. Phylogenetic analyses

Subsequently, the phylogenetic analysis was performed with amino acid sequences of galectin-3 proteins from species of fish and mammals, using the neighbor-joining method in MEGA 6. In our results, *Sm*Lgals3 was firstly clustered with fugu, and then clustered with tilapia, medeka, and zebrafish (Fig. 2). The higher vertebrates formed single clade including human, mouse, chicken and green sea turtle (Fig. 2). And all branching nodes were supported by high bootstrap values.

3.4. Syntenic analysis

Finally, the syntenic analysis was performed for further validation of the identification of *Sm*Lgals3 gene. In general, a relatively conserved synteny was observed in comparison of *Sm*Lgals3 to other species. After searching the genomic databases of different species, the same neighboring genes were found across the selected species, including CDKN3, CNIH1, GMFB, L2HGDH, MED6, SOS2, and ACTN1 (Fig. 3).

3.5. The tissue distribution of SmLgals3

The tissue distribution of *Sm*Lgals3 was examined in eight turbot healthy tissues by real-time PCR method. In our results, *Sm*Lgals3 was widely expressed in all the examined tissues, with the highest expression level in brain (46.28 fold), followed by intestine (12.6 fold), head-kidney (7.15 fold) and blood (6.2 fold), while the lowest expression level was detected in skin (Fig. 4).

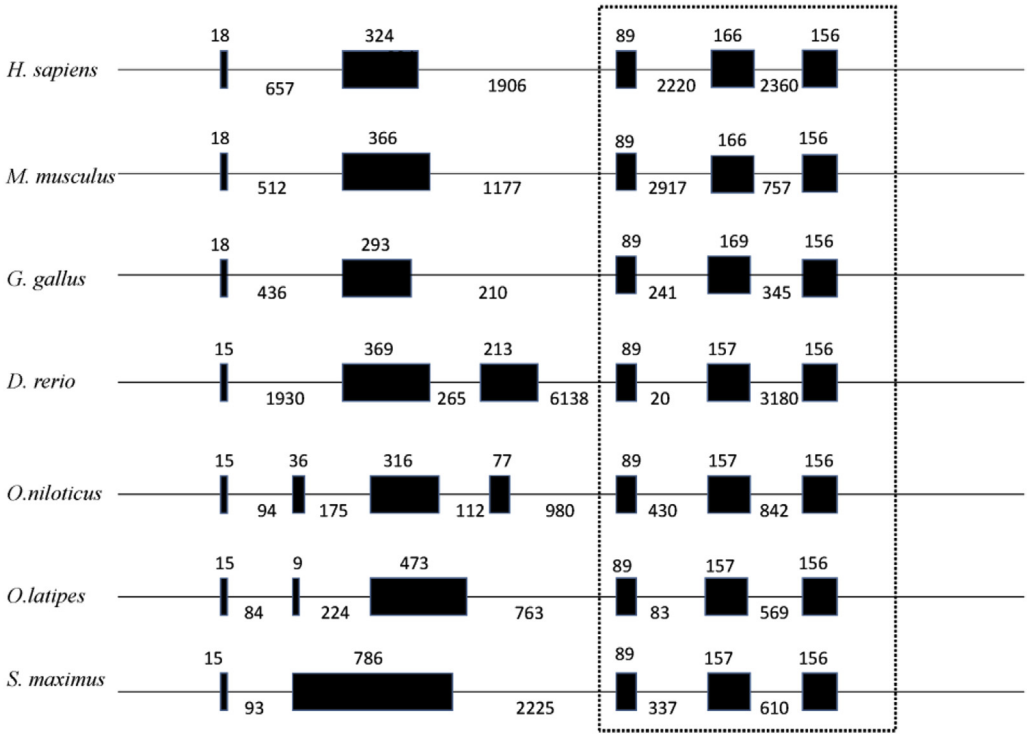

Fig. 1. Exon/intron organization of *Sm*Lgals3 gene was obtained by using Splign to align cDNA sequence to the turbot genome. Boxes indicate exons and dashes indicate introns. The dark shaded boxes indicate exon sequences that encoding amino acids.

3.6. Expression profiles of SmLgals3 following bacterial challenge

In order to characterize the immune roles of *Sm*Lgals3 in turbot mucosal immunity, the expression profiles of *Sm*Lgals3 were investigated in mucosal tissues (gill, skin and intestine) at early time-points following immersion challenge with Gram-negative bacteria *V. anguillarum*, and Gram-positive bacteria *S. iniae*, respectively.

Following *V. anguillarum* challenge, *Sm*Lgals3 was significantly down-regulated in all the three tissues except up-regulated in skin with 12.36 fold at 2 h, but it was quickly down-regulated with −4.65 fold at 6 h, and then returned to basal level (Fig. 5). The most up-regulation was detected in intestine at 6 h with −28.19 fold, and −6.59 fold at 12 h. Different from other tissues, the gill showed −3.58 fold at 6 h, −9.64 fold at 12 h, and the most dramatic down-regulation at 24 h with −22.99 fold (Fig. 5).

In *S. iniae* challenge, the *Sm*Lgals3 was down-regulated much more quickly than that in *V. anguillarum* challenge. The *Sm*Lgals3 was down-regulated at 2 h in all the three tissues, with −13.01 fold in intestine, −10.78 fold in skin, and −3.43 fold in gill (Fig. 6). Interestingly, it quickly returned to basal level in gill and skin, while continued to be down-regulated in intestine with −9.58 fold at 8 h and −15.46 fold at 12 h (Fig. 6).

3.7. Microbial ligand-binding in vitro

The binding ability of *Sm*Lgals3 to microbial ligands was investigated to further characterize its function. Briefly, the *rSm*Lgals3 was purified from *E. coli* as a native His-tagged protein. In SDS-PAGE analysis, only a single band was observed (Supplementary Fig. 1). In our results, the strong binding ability was observed to LPS, PGN and LTA (Fig. 7). The strongest binding ability was detected to LPS which showed significant binding ability at 0.5 μg/ml, while the significant binding ability for PGN was observed at 0.5μg/ml, and 2.0 μg/mL for LTA (Fig. 7).

4. Discussion

Galectins are widely distributed in primary and secondary lymphoid organs and many types of immune cells, with vital roles in regulation of immune cell proliferation and apoptosis [27]. A growing body of

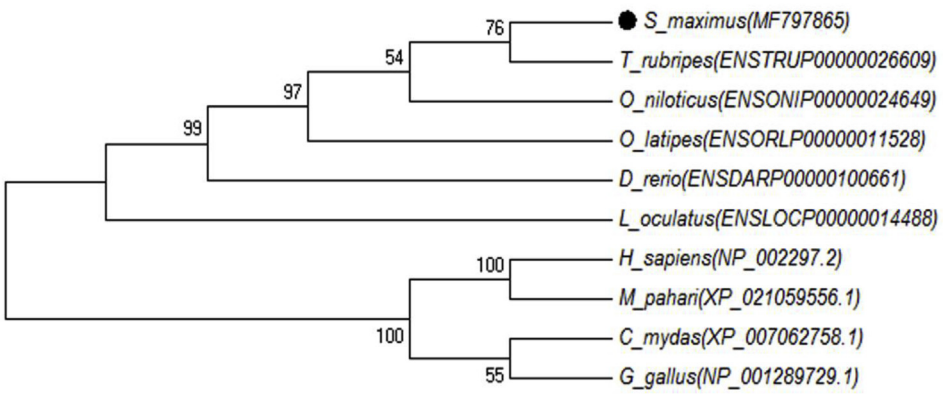

Fig. 2. Phylogenetic tree for the *Sm*Lgals3 gene. The phylogenetic tree was constructed based on the amino acid sequences of *Sm*Lgals3 from different species using the neighbor-joining method in MEGA 6. Gaps were removed by complete deletion and the phylogenetic tree was evaluated with 1000 bootstrap replications. Dark solid circles indicated the newly characterized *Sm*Lgals3 gene.

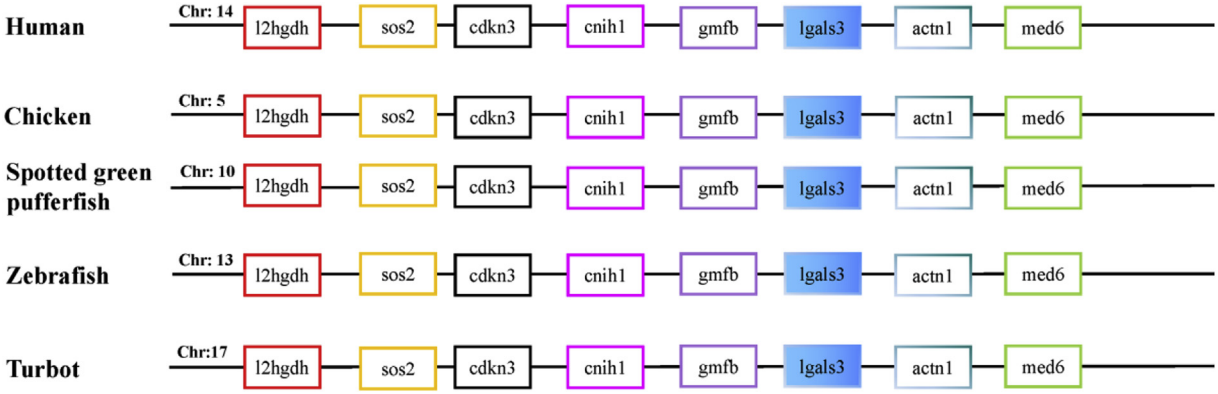

Fig. 3. Syntenic analysis of galectin-3 genes from turbot, human, chicken, tetraoden, zebrafish, medaka, spotted gar, fugu. The galectin-3 gene is highlighted by bright blue color filled boxes. CDKN3: Cyclin-dependent kinase inhibitor 3; CNIH1: cornichon family AMPA receptor auxiliary protein 1; GMFB: Glia maturation factor beta; L2HGDH: L-2-hydroxyglutarate dehydrogenase; MED6: mediator complex subunit 6; SOS2: Ras/Rho guanine nucleotide exchange factor 2; ACTN1:actinin alpha 1. (For interpretation of the references to color in this figure legend, the reader is referred to the Web version of this article.)

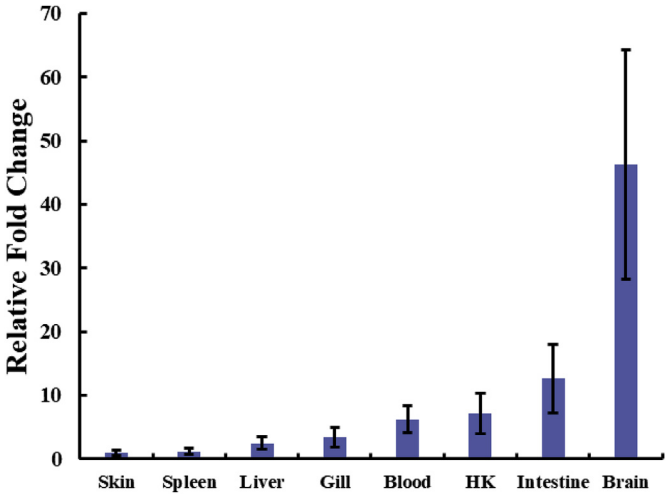

Fig. 4. The tissue distribution of *Sm*Lgals3 in turbot. The expression levels of *Sm*Lgals3 in liver, skin, spleen, blood, head kidney, intestine, gill and brain were determined by quantitative real-time PCR. The expression level of *Sm*Lgals3 in skin was set as 1. The relative abundance of *Sm*Lgals3 was expressed as mean ± SE (N = 3).

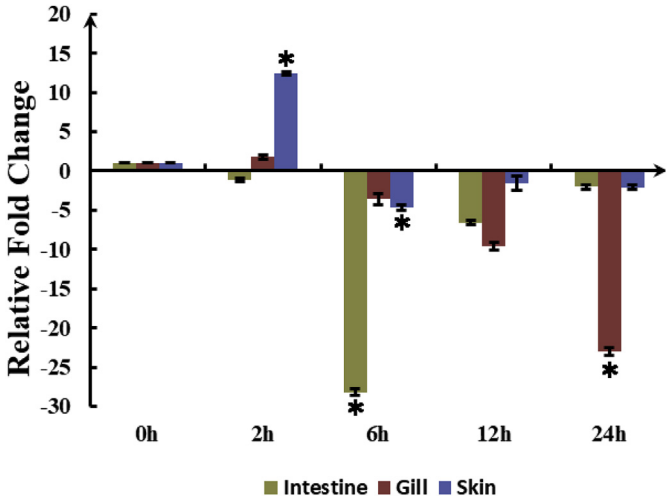

Fig. 5. The expression patterns of *Sm*Lgals3 in turbot tissues at different timepoints (2 h, 6 h, 12 h, and 24 h) after *V. anguillarum* challenge. The expression levels of *Sm*Lgals3 in skin, intestine and gill were determined by quantitative real-time PCR. 18S rRNA was employed as an internal control. Asterisks (*) marked the significant differences between experimental and control group ($P < 0.05$). Error bars indicated standard error (n = 3).

evidence have indicated galectin-3 could involve in chemotaxis, phagocytosis, LPS-induced IL-1 production, NADPH-oxidase activity, and IL-4 induced survival of memory B cells [28–30]. Although considerable experimental evidences have elucidated galectin functions within the immune system in higher mammals, the characterization of galectin-3 is still lacking in teleost species. Here, we identified galectin-3 gene in turbot, performed expression profiling analysis of galectin-3 in response to different bacterial infection, as well as the binding ability analysis to different microbial ligands, to provide initial information for further functional characterization of galectin-3 in teleost. In this study, one galectin-3 gene was captured in turbot (*Sm*Lgals3) with similar molecular properties to other fish species (Table 1). As an evolutionarily highly conserved family of proteins, the genomic structure analysis, phylogenetic analysis and synteny analysis validated the identification of *Sm*Lgals3 and showed the strong orthology to their counterparts vertebrate species.

In tissue distribution analysis, *Sm*Lgals3 was widely expressed in all the examined tissues, with the highest expression level in brain, followed by intestine (Fig. 4). Interestingly, galectin-3 was reported to be widely expressed in rat brain, and seems to be regulated by developmental cascades [31], also was considered as mediator of microglia responses in injured brain [32]. In addition, galectin-3 was highly expressed in the colons of patients with ulcerative colitis [33]. However, galectin-3 was highly expressed in gill and skin, and lowly expressed in intestine in catfish [34], while it showed the lowest expression level in skin in turbot. With the limited information about expression profiling of galectin-3 in teleost, the putative roles of galectin-3 in different tissues of teleost need to be further characterized.

Subsequently, the expression patterns of *Sm*Lgals3 were characterized following different bacteria challenge in order to gain insight into its immune roles in mucosal immunity. Notably, *Sm*Lgals3 showed significant down-regulation in all the tissues following both Gram-negative bacteria *V. anguillarum*, and Gram-positive bacteria *S. iniae* challenge, with the most down-regulation in intestine. Previously, *V. anguillarum* cells were detected in spleens from more than 50% of orally or rectally infected fish, suggesting that the intestine might serving as a portal of entry for *V anguillarum* [35]. Following orally administered *V. anguillarum* in turbot, the bacteria showed strong ability to survive in the acidic environment of the stomach, and persist in the intestine, which suggested that the turbot intestinal tract could serve as an enrichment site for *V. anguillarum* [36]. In zebrafish, the entry of *V. anguillarum* through the mouth into the intestine was detected at 2 h following bath challenge with *V. anguillarum*, and the localisation of *V.*

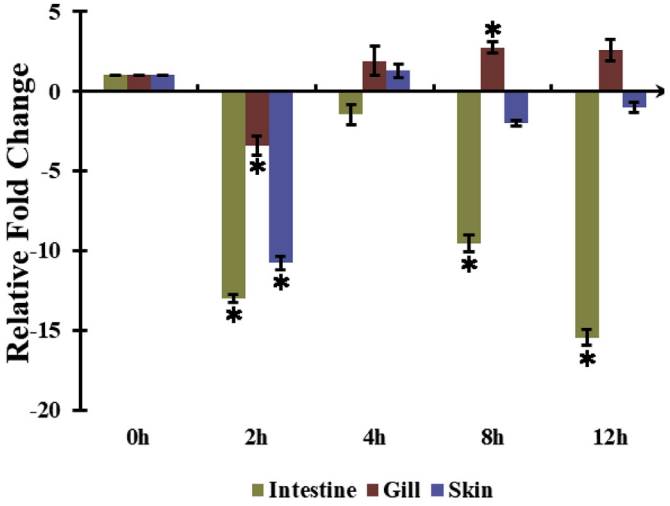

Fig. 6. The expression patterns of *Sm*Lgals3 in turbot mucosal tissues at different timepoints (2 h, 4 h, 8 h, and 12 h) after *S. iniae* challenge. The expression levels of *Sm*Lgals3 in skin, intestine and gill were determined by quantitative real-time PCR. 18S rRNA was employed as an internal control. Asterisks (*) marked the significant differences between experimental and control group ($P < 0.05$). Error bars indicated standard error (n = 3).

anguillaum was detected in intestine at 6 h [37]. Moreover, following bath-vaccination of live attenuated *V. anguillarum* vaccine, bacteria cells proliferated rapidly in 3 h after vaccination and maintained at a high level until 6 h in the intestine, with a significant up-regulation of TLR5 triggering MyD88-dependent signaling pathway in the intestine [38]. Comparing to *V. anguillarum* challenge, *Sm*Lgals3 was significantly down-regulated in all the timepoints in the intestine following *S. iniae* challenge. In Japanese flounder, the *S. iniae* bath challenge could induce much more significant deaths in lower concentration than oral challenge [39]. Previously, several immune-related genes were also significantly up-regulated following *S. iniae* infection in turbot intestine [14–16]. In contrast, galectin-3 was significantly up-regulated in catfish skin following *Aeromonas hydrophila* infection [40]. Although our knowledge of galectin-3 are limited in fish, it has been well documented in mammalian species. For instance, In gastric epithelial cells, galectin-3 was up-regulated following *Helicobacter pylori* infection [41]. Galectin-3 showed inhibition effect on the colonic mucosa inflammation and reduced disease severity by inducing regulatory T cells [42]. Galectin-3 deletion resulted in the suppressed production of pro-inflammatory cytokines in colonic macrophages and favored their alternative activation, as well as significantly reduced activation of NOD-like receptor family in macrophages [33]. Several studies following different bacteria challenge, suggested that galectin-3 might act as a cell surface docking site or a cross-linking molecule promoting adhesion [43–46]. Further work is warranted to examine whether turbot galectin-3 may play similar roles in supporting pathogen adhesion.

As typical lectins, galectins possessed carbohydrate binding ability to microbial pathogens by recognizing exogenous ligands, especially carbohydrates on the surface of microbes via their CRDs, and subsequently trigger downstream immune signaling pathways to eliminate the pathogens. The structure features might affect their specificity and binding affinity to carbohydrates. As the only member of chimera type galectins, galectin-3 should have different immune functions compared to proto and tandem-repeat type lectins. Here, r*Sm*Lgals3 showed strong binding ability to LPS and PGN, followed by LTA. In *Crassostrea gigas*, galectin-3 showed the highest affinity to PGN, as well as Gram-positive bacteria, Gram-negative bacteria and fungi [13]. However, galectin-2 (proto type) did not bind to LPS, PGN, or glucan, while it could bind Gram-negative bacteria and fungi in *Crassostrea gigas* [13].

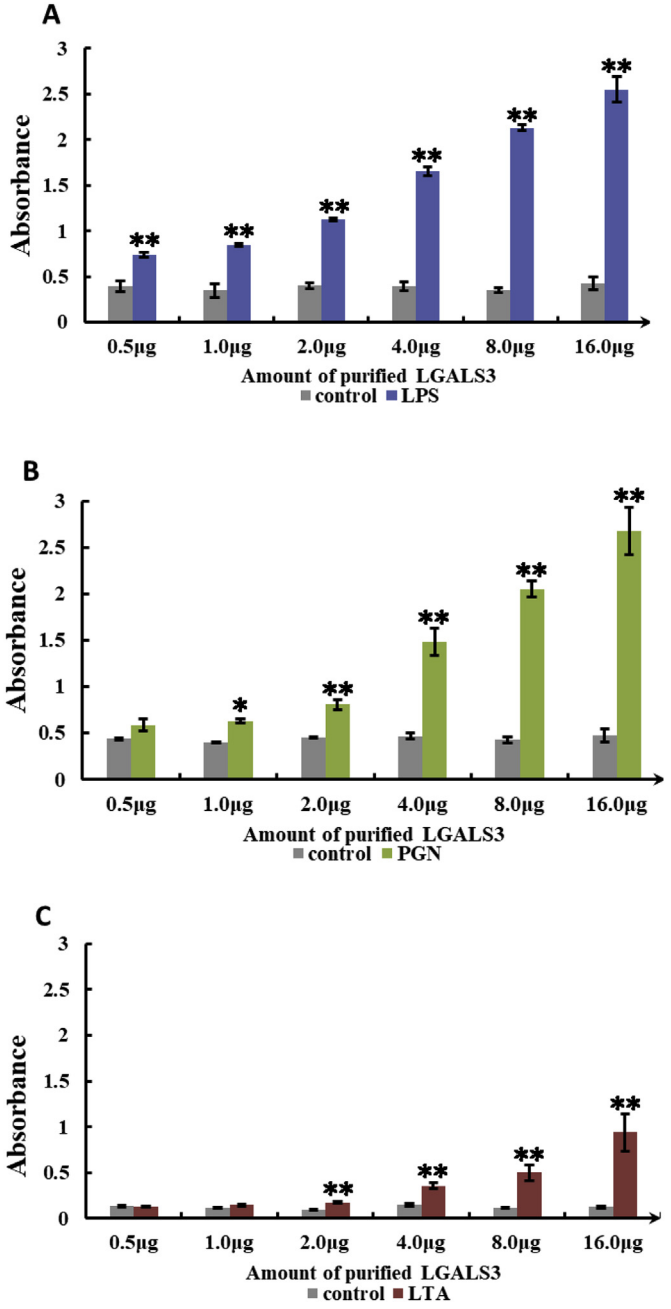

Fig. 7. Results of the *in vitro* binding assay of *Sm*Lgals3 to microbial ligands, including lipopolysaccharide, peptidoglycan, and lipoteichoic acid. * indicate a significant difference in the absorbance between different microbial ligands that exposed to r*Sm*Lgals3 and the control group: *p < 0.05; **p < 0.01.

In addition, recombinant galectin-3 could also function like a chemokine to induce the migration of monocytes and macrophages in human [47]. As serving as a bridge between the cell and the extracellular matrix to promote adhesion, recombinant galectin-3 could increase the adhesive properties of human neutrophils to laminin [48].

Notably, galectin-3 possessed a unique feature to oligomerize after glycoprotein binding at the cell surface, with the N terminus self-association domain [48]. In this regard, galectin-3 has been reported to influence the stability of cell-cell adhesion matrix to involve in many biological processes with other genes [49]. Especially, galectin-3 was reported to contribute to epithelial barrier integrity. For example, galectin-3 could regulate the barrier function of the intestinal epithelium by controlling Desmoglein-2 protein stability and intercellular adhesion

[50]. In gastric epithelial cells, knock down of galectin-3 led to reduced NF-κB promoter activity and interleukin-8 (IL-8) secretion, suggesting its pro-inflammatory roles [41]. In airway epithelial cells, galectin-3 was reported to regulate inflammatory response by modulating the expression of SOCS1 and RIG1 [51]. Taken together, galectin-3 plays vital roles in mucosal homeostasis and barrier maintenance. However, the knowledge of galectin-3 are still limited in teleost species, further studies should be carried out to better characterize its detailed roles in teleost mucosal immunity.

Acknowledgement

This study was supported by the National Science Foundation of China (No.:31602193). And it was also supported by keypoint research and invention program in Shandong Province (2017GHY215004).

Appendix A. Supplementary data

Supplementary data to this article can be found online at https://doi.org/10.1016/j.fsi.2018.10.009.

References

[1] H. Leffler, S. Carlsson, M. Hedlund, Y. Qian, F. Poirier, Introduction to galectins, Glycoconj. J. 19 (7–9) (2004) 433.
[2] D.N. Cooper, Galectinomics: finding themes in complexity, Biochim. Biophys. Acta Gen. Subj. 1572 (2) (2002) 209–231.
[3] C. Li, X. Wei, X. Li, Galectins-structure and function of galectins, Prog. Veterinary Med. 24 (2003).
[4] J. Hirabayashi, K. Kasai, The family of metazoan metal-independent beta-galactoside-binding lectins: structure, function and molecular evolution, Glycobiology 3 (4) (1993) 297–304.
[5] L. Johannes, R. Jacob, H. Leffler, Galectins at a glance, J. Cell Sci. 131 (9) (2018) jcs208884.
[6] V.I. Teichberg, I. Silman, D.D. Beitsch, G. Resheff, A β -D-galactoside binding protein from electric organ tissue of electrophorus electricus, Proc. Natl. Acad. Sci. U.S.A. 72 (4) (1975) 1383–1387.
[7] S. Zhou, H. Zhao, W. Thongda, D. Zhang, B. Su, D. Yu, E. Peatman, C. Li, Galectins in channel catfish, Ictalurus punctatus: characterization and expression profiling in mucosal tissues, Fish Shellfish Immunol. 49 (2016) 324–335.
[8] Y. RY, R. GA, L. FT, Galectins: structure, function and therapeutic potential, Expet Rev. Mol. Med. 10 (article e17) (2015) e17.
[9] S.M. B, N. A, G. M, B. S, V. L, K. M, M. S, M. M, B. G, T. V, Gal-3 plays an important pro-inflammatory role in the induction phase of acute colitis by promoting activation of NLRP3 inflammasome and production of IL-β in macrophages, J. Crohns & Colitis 10 (5) (2016) 593.
[10] D.K. Hsu, S.R. Hammes, I. Kuwabara, W.C. Greene, F.T. Liu, Human T lymphotropic virus-I infection of human T lymphocytes induces expression of the beta-galactoside-binding lectin, galectin-3, Am. J. Pathol. 148 (5) (1996) 1661–1670.
[11] M.A. Toscano, G.A. Bianco, J.M. Ilarregui, D.O. Croci, J. Correale, J.D. Hernandez, N.W. Zwirner, F. Poirier, E.M. Riley, L.G. Baum, Differential glycosylation of TH1, TH2 and TH-17 effector cells selectively regulates susceptibility to cell death, Nat. Immunol. 8 (8) (2007) 825–834.
[12] M. NitaLazar, J. Mancini, C. Feng, C. Ravindran, S. Jackson, A.d.l. HerasSánchez, B. Giomarelli, H. Ahmed, S.M. Haslam, G. Wu, The zebrafish galectins Drgal1-L2 and Drgal3-L1 bind in vitro to the infectious hematopoietic necrosis virus (IHNV) glycoprotein and reduce viral adhesion to fish epithelial cells, Dev. Comp. Immunol. 55 (5) (2016) 241–252.
[13] M. Huang, T. Zhou, Y. Wu, H. Fei, G. Wang, Z. Li, Y. Lei, Q. Liu, C. Sun, Z. Lv, Characterisation and functional comparison of single-CRD and multidomain containing galectins CgGal-2 and CgGal-3 from oyster Crassostrea gigas, Fish Shellfish Immunol. (2018) 1–9.
[14] L. Zhang, C. Gao, F. Liu, L. Song, B. Su, C. Li, Characterization and expression analysis of a peptidoglycan recognition protein gene, SmPGRP2 in mucosal tissues of turbot (Scophthalmus maximus L.) following bacterial challenge, Fish Shellfish Immunol. 56 (2016) 367.
[15] X. Dong, B. Su, S. Zhou, M. Shang, H. Yan, F. Liu, C. Gao, F. Tan, C. Li, Identification and expression analysis of toll-like receptor genes (TLR8 and TLR9) in mucosal tissues of turbot (Scophthalmus maximus L.) following bacterial challenge, Fish Shellfish Immunol. 58 (2016) 309–317.
[16] X. Dong, Q. Fu, S. Liu, C. Gao, B. Su, F. Tan, C. Li, The expression signatures of neuronal nitric oxide synthase (NOS1) in turbot (Scophthalmus maximus L.) mucosal surfaces against bacterial challenge, Fish Shellfish Immunol. 59 (2016) 406–413.
[17] C. Gao, Q. Fu, S. Zhou, S. Lin, Y. Ren, X. Dong, B. Su, C. Li, The mucosal expression signatures of g-type lysozyme in turbot (Scophthalmus maximus) following bacterial challenge, Fish Shellfish Immunol. 54 (2016) 612.
[18] F. Liu, B. Su, C. Gao, S. Zhou, L. Song, F. Tan, X. Dong, Y. Ren, C. Li, Identification and expression analysis of TLR2 in mucosal tissues of turbot (Scophthalmus maximus L.) following bacterial challenge, Fish Shellfish Immunol. 55 (2016) 654.
[19] C. Gao, F. Qiang, B. Su, S. Zhou, F. Liu, S. Lin, Z. Min, Y. Ren, X. Dong, F. Tan, Transcriptomic profiling revealed the signatures of intestinal barrier alteration and pathogen entry in turbot (Scophthalmus maximus) following Vibrio anguillarum challenge, Dev. Comp. Immunol. 65 (2016) 159–168.
[20] M.R. Wilkins, E. Gasteiger, A. Bairoch, J.C. Sanchez, K.L. Williams, R.D. Appel, D.F. Hochstrasser, Protein identification and analysis tools in the ExPASy server, Methods Mol. Biol. 112 (112) (1999) 571–607.
[21] Y. Kapustin, A. Souvorov, T. Tatusova, D. Lipman, Splign: algorithms for computing spliced alignments with identification of paralogs, Biol. Direct 3 (1) (2008) 20.
[22] F. Sievers, A. Wilm, D. Dineen, T.J. Gibson, K. Karplus, W. Li, R. Lopez, H. Mcwilliam, M. Remmert, J. Söding, F. Sievers, A. Wilm, D. Dineen, T.J. Gibson, K. Karplus, W. Li, et al., Fast, scalable generation of high-quality protein multiple sequence alignments using Clustal Omega, Mol. Syst. Biol. 7 (1) (2011) 539.
[23] K. Tamura, G. Stecher, D. Peterson, A. Filipski, S. Kumar, MEGA6: molecular evolutionary Genetics analysis version 6.0, Mol. Biol. Evol. 30 (12) (2013) 2725.
[24] M. Muffato, A. Louis, C.E. Poisnel, H.R. Crollius, Genomicus, Bioinform. 26 (8) (2010).
[25] M.W. Pfaffl, G.W. Horgan, L. Dempfle, Relative expression software tool (REST) for group-wise comparison and statistical analysis of relative expression results in real-time PCR, Nucleic Acids Res, Nucleic acids research 30 (9) (2002) e36-e36(1).
[26] A. Figueras, D. Robledo, A. Corvelo, M. Hermida, P. Pereiro, J.A. Rubiolo, J. Gómezgarrido, L. Carreté, X. Bello, M. Gut, Whole genome sequencing of turbot (Scophthalmus maximus; Pleuronectiformes): a fish adapted to demersal life, DNA Res. 23 (3) (2016) 181–192 23,3(2016-3-6).
[27] G.A. Rabinovich, L.G. Baum, N. Tinari, R. Paganelli, C. Natoli, F.T. Liu, S. Iacobelli, Galectins and their ligands: amplifiers, silencers or tuners of the inflammatory response? Trends Immunol. 23 (6) (2002) 313–320.
[28] N. Rubinstein, J.M. Ilarregui, M.A. Toscano, G.A. Rabinovich, The role of galectins in the initiation, amplification and resolution of the inflammatory response, Tissue Antigens 64 (1) (2004) 1–12.
[29] R.Y. Yang, D.K. Hsu, F.T. Liu, Expression of galectin-3 modulates T-cell growth and apoptosis, Proc. Natl. Acad. Sci. U.S.A. 93 (13) (1996) 6737–6742.
[30] T. Fukumori, Y. Takenaka, T. Yoshii, H.R.C. Kim, V. Hogan, H. Inohara, S. Kagawa, A. Raz, CD29 and CD7 mediate galectin-3-induced type II T-cell apoptosis, Cancer Res. 63 (23) (2003) 8302–8311.
[31] H.I. Yoo, E.G. Kim, E.J. Lee, S.Y. Hong, C.S. Yoon, M.J. Hong, S.J. Park, R.S. Woo, T.K. Baik, D.Y. Song, Neuroanatomical distribution of galectin-3 in the adult rat brain, J. Mol. Histol. 48 (2) (2017) 133–146.
[32] R. Rahimian, L.C. Béland, J. Kriz, Galectin-3: mediator of microglia responses in injured brain, Drug Discov. Today 23 (2) (2017).
[33] B.S. Markovic, A. Nikolic, M. Gazdic, S. Bojic, L. Vucicevic, M. Kosic, S. Mitrovic, M. Milosavljevic, G. Besra, V. Trajkovic, Galectin-3 plays an important pro-inflammatory role in the induction phase of acute colitis by promoting activation of NLRP3 inflammasome and production of IL-1β in macrophages, Journal of Crohns & Colitis 10 (5) (2016) 593.
[34] S. Zhou, H. Zhao, W. Thongda, D. Zhang, B. Su, Y. Dan, E. Peatman, L. Chao, Galectins in channel catfish, Ictalurus punctatus : characterization and expression profiling in mucosal tissues, Fish Shellfish Immunol. 49 (2016) 324–335.
[35] J.C. Oisson, A. Jöborn, A. Westerdahl, L. Blomberg, S. Kjelleberg, P.L. Conway, Is the turbot, Scophthalmus maximus (L.), intestine a portal of entry for the fish pathogen Vibrio anguillarum? J. Fish. Dis. 19 (3) (2010) 225–234.
[36] Jöborn Olsson, Blomberg Westerdahl, Conway Kjelleberg, Survival, persistence and proliferation of Vibrio anguillarum in juvenile turbot, Scophthalmus maximus (L.), intestine and faeces, J. Fish. Dis. 21 (1) (2010) 1–9.
[37] R. O'Toole, H.J. Von, R. Rosqvist, P.E. Olsson, H. Wolfwatz, Visualisation of zebrafish infection by GFP-labelled Vibrio anguillarum, Microb. Pathog. 37 (1) (2004) 41–46.
[38] X. Liu, H. Wu, X. Chang, Y. Tang, Q. Liu, Y. Zhang, Notable mucosal immune responses induced in the intestine of zebrafish (Danio rerio) bath-vaccinated with a live attenuated Vibrio anguillarum vaccine, Fish Shellfish Immunol. 40 (1) (2014) 99–108.
[39] N.H. Thinh, Immunohistochemical examination of experimental Streptococcus iniae infection in Japanese flounder Paralichthys olivaceus, Fish Pathol. 36 (3) (2009) 40–41.
[40] C. Li, R. Wang, B. Su, Y. Luo, J. Terhune, B. Beck, E. Peatman, Evasion of mucosal defenses during Aeromonas hydrophila infection of channel catfish (Ictalurus punctatus) skin, Dev. Comp. Immunol. 39 (4) (2013) 447–455.
[41] V.V. Subhash, B. Ho, Galectin 3 acts as an enhancer of survival responses in H. pylori-infected gastric cancer cells, Cell Biol. Toxicol. 32 (1) (2016) 23–35.
[42] H.F. Tsai, C.S. Wu, Y.L. Chen, H.J. Liao, I.T. Chyuan, P.N. Hsu, Galectin-3 suppresses mucosal inflammation and reduces disease severity in experimental colitis, J. Mol. Med. 94 (5) (2016) 545–556.
[43] E. Altman, B.A. Harrison, R.K. Latta, K.K. Lee, J.F. Kelly, P. Thibault, Galectin-3-mediated adherence of Proteus mirabilis to Madin-Darby canine kidney cells, Biochem. Cell Biol.-biochimie Et Biologie Cellulaire 79 (6) (2001) 783–788.
[44] M. Fowler, R.J. Thomas, J. Atherton, I.S. Roberts, N.J. High, Galectin-3 binds to Helicobacter pylori O-antigen: it is upregulated and rapidly secreted by gastric epithelial cells in response to H-pylori adhesion, Cell Microbiol. 8 (1) (2006) 44–54.
[45] R.S. Gupta, V. Bhandari, Phylogeny and molecular signatures for the phylum Thermotogae and its subgroups, Antonie Leeuwenhoek 100 (1) (2011) 1–34.
[46] P. Quattroni, Y. Li, D. Lucchesi, S. Lucas, D.W. Hood, M. Herrmann, H.J. Gabius, C.M. Tang, R.M. Exley, Galectin-3 binds Neisseria meningitidis and increases interaction with phagocytic cells, Cell Microbiol. 14 (11) (2012) 1657–1675.
[47] R.Y. Yang, G.A. Rabinovich, F.T. Liu, Galectins: structure, function and therapeutic potential, Expet Rev. Mol. Med. 10 (article e17) (2015) e17.

[48] I. Kuwabara, F.T. Liu, Galectin-3 promotes adhesion of human neutrophils to laminin, J. Immunol. 156 (10) (1996) 3939–3944.
[49] H. Inohara, A. Raz, Functional evidence that cell surface galectin-3 mediates homotypic cell adhesion, Cancer Res. 55 (15) (1995) 3267.
[50] K. Jiang, C.R. Rankin, P. Nava, R. Sumagin, R. Kamekura, S.R. Stowell, M. Feng, C.A. Parkos, A. Nusrat, Galectin-3 regulates desmoglein-2 and intestinal epithelial intercellular adhesion, J. Biol. Chem. 289 (15) (2014) 10510–10517.
[51] N.L. Mihai, B. Aditi, F. Chiguang, G.R. Vasta, Galectins regulate the inflammatory response in airway epithelial cells exposed to microbial neuraminidase by modulating the expression of SOCS1 and RIG1, Mol. Immunol. 68 (2) (2015) 194–202.